The Astrophysical Journal, 669:952–958, 2007 November 10

THE PRESSURE-CONFINED WIND OF THE MASSIVE AND COMPACT SUPER STAR CLUSTER M82-A1

Sergiy Silich and Guillermo Tenorio-Tagle
Instituto Nacional de Astrofísica Optica y Electrónica, AP 51, 72000 Puebla, Mexico; silich@inaoep.mx

and

Casiana Muñoz-Tuñón
Instituto de Astrofísica de Canarias, E 38200 La Laguna, Tenerife, Spain; cmt@ll.iac.es
Received 2007 June 7; accepted 2007 July 18

ABSTRACT

The observed parameters of the young super star cluster M82-A1 and its associated compact H II region are here shown to indicate a low heating efficiency or immediate loss, through radiative cooling, of a large fraction of the energy injected by stellar winds and supernovae during the early evolution of the cluster. This implies a bimodal hydrodynamic solution, which leads to a reduced mass deposition rate into the ISM, with a much reduced outflow velocity. We also show here that in order to match the observed parameters of the H II region associated with M82-A1, the resulting star cluster wind should be confined by a high-pressure interstellar medium. The cluster wind parameters, together with the location of the reverse shock, its cooling length, and the radius of the standing outer H II region, are derived analytically. All of these properties are then confirmed with a semianalytical integration of the flow equations, which provides also us with the run of the hydrodynamic variables as a function of radius. The impact of the results is discussed and extended to other massive and young super star clusters surrounded by a compact H II region.

Subject headings: galaxies: individual (M82) — galaxies: star clusters — H II regions — ISM: bubbles — ISM: individual (M82-A1)

1. INTRODUCTION

In many starburst, interacting, and merging galaxies, a substantial fraction of star formation is concentrated in a number of compact ($R_{SC} \leq 10$ pc), young (a few $\times 10^6$ yr), and massive ($10^5 \leq M_{SC} \leq 10^6$) stellar clusters (super star clusters; SSCs). These entities may represent the dominant sites of star formation in these galaxies (McCrady et al. 2003; Whitmore 2003), and if held by gravity they also represent the earliest stages of globular cluster evolution (Muñoz-Tuñón et al. 2004). Their large UV photon output and their powerful, high-velocity gaseous outflows (the star cluster winds) are now believed to be the major agents responsible for the large-scale structuring of the interstellar medium (ISM) and for the dispersal of heavy elements within their host galaxies and the intergalactic medium (IGM).

M82-A1 is one of these SSCs in the galaxy M82 (Smith et al. 2006), with a half-light radius $R_{SC} = 3 \pm 0.5$ pc, an age $\tau_{SC} = 6.4 \pm 0.5$ Myr, a UV photon output $N^{tot} = (7.5 \pm 3.0) \times 10^{50}$ s^{-1}, and a mass $M_{SC} = (1.3 \pm 0.5) \times 10^6\ M_\odot$ if one assumes an IMF with a Salpeter slope and 0.1 $M_\odot$ and 100 $M_\odot$ as the lower and upper mass cutoffs. Stellar evolution synthesis models (such as Starburst99; see Leitherer et al. 1999) predict an average mechanical energy input rate for M82-A1 equal to $L_{SC} = 2.5 \times 10^{40}$ erg s^{-1}. Given such a large energy deposition rate, it seems surprising that M82-A1 is, after such an evolution time, still surrounded by a compact H II region, with a radius $R_{H\,II} = 4.5$ pc, a density $n_{H\,II} \approx 1800$ cm^{-3}, a metallicity $\sim$1–2 times solar, and a total mass of only 5000 $M_\odot$, instead of having produced a large-scale superbubble. Note that a similar argument can be made for many of the SSCs embedded in the 150 pc nuclear region of M82 (see de Grijs et al. 2001; Melo et al. 2005), as well as for a number of the extragalactic H II regions (Kewley & Dopita 2002; Dopita et al. 2005).

Smith et al. (2006) suggested that the H II region associated with M82-A1 may result from the photoionization of a 4.5 pc shell blown into the ISM by the central cluster. However, as the observed size of the H II region is not consistent with the standard bubble model (see Weaver et al. 1977; Bisnovatyi-Kogan & Silich 1995, and references therein), they assumed that the kinetic energy of the photoionized shell represents only a small fraction ($\sim$0.1) of the mechanical energy, L_{SC}, released inside the cluster, and that the high pressure of the ambient medium has reduced the expansion velocity to 30 km s^{-1}, the FWHM of the observed emission lines.

This scenario, although intuitively correct, rises several questions. First, the spectrophotometric age of the cluster, $\tau_{SC} \approx 6.4$ Myr (Smith et al. 2006), is inconsistent with the kinematic age of the shell (τ_k), even if one assumes 30 km s^{-1} as the expansion speed throughout its evolution, $\tau_k = R_{H\,II}/V_{exp} \approx 1.5 \times 10^5$ yr. Second, if the matter injected by supernovae (SNe) and stellar winds is accumulated inside the H II radius, $R_{H\,II} = 4.5$ pc, then the gas number density should be $n_{H\,II} > 3L_{SC}\tau_{SC}/2\pi\mu V_\infty^2 R_{H\,II}^3 \approx 2.7 \times 10^4$ cm^{-3}, where μ is the mean mass per ion, and a wind terminal speed $V_\infty = 1000$ km s^{-1} was assumed. This density is an order of magnitude larger than that found in the H II region. Note also that only a small fraction, $f_{H\,II} < 0.001$, of this gas could be photoionized by M82-A1, and thus, in this interpretation, a good fraction of the mass supplied by supernovae explosions and stellar winds is hidden somewhere within the 4.5 pc volume. These arguments imply that the cluster and H II region parameters are not consistent with the wind-driven bubble model.

In order to have a consistent model, here we look at the detailed hydrodynamics of the gas reinserted by winds and supernovae within the cluster volume. The original adiabatic star cluster wind model, proposed by Chevalier & Clegg (1985), described various assumptions that have been used by all subsequent modelers, such as equal spacing between sources within the SSC volume, and that random collisions of the ejecta from nearby stellar winds and supernova explosions would result in a full thermalization of the matter reinserted by the evolving sources. Under such conditions, the pressure of the thermalized matter would exceed that of the surrounding ISM, and the injected gas would

be accelerated to leave the cluster with a high velocity, while establishing a stationary wind. For this to happen, the gas has to acquire a particular velocity distribution, increasing almost linearly with radius from the stagnation point, the place where the gas velocity is equal to 0 km s^{-1}, which occurs at the cluster center, to the sound speed, c_{SC}, that should occur at the cluster surface. Outside of the cluster, pressure gradients would allow the wind to reach its terminal speed ($v_\infty \approx 2c_{SC}$).

The observed parameters of SSCs (Ho 1997; Whitmore 2003; Turner et al. 2003; Turner & Beck 2004; Pasquali et al. 2004; Melo et al. 2005; Walcher et al. 2005; Martín Hernández et al. 2005; Thompson et al. 2006; Larsen 2006, and references therein) led us however, to reanalyze the original adiabatic model of Chevalier & Clegg (1985) and to realize that in the case of massive and compact star clusters, radiative cooling may crucially affect the internal structure and the hydrodynamics of the flow (Silich et al. 2004). In a more recent communication, Tenorio-Tagle et al. (2007) have shown that if the mechanical luminosity of a cluster exceeds a critical value (the threshold line), then a bimodal hydrodynamic solution for the matter reinserted by winds and SNe is established. In such cases, the densest central regions within the cluster volume undergo strong radiative cooling, which depletes the energy available for the cluster wind. This also moves the stagnation radius, R_{st}, out of the cluster center, and promotes the accumulation and reprocessing of the enclosed matter into further generations of stars (Tenorio-Tagle et al. 2005). Meanwhile, the matter injected between the stagnation radius and the cluster surface is still able to drive a stationary wind. This, however, cools rapidly at a short distance from the cluster surface and becomes exposed to the UV radiation escaping the cluster. Wünsch et al. (2007) has also shown that the location of the threshold line that separates clusters evolving in the bimodal regime from those with the stagnation point at the star cluster center, which are thus able to eject all of the deposited mass out of the cluster, can be well approximated by simple analytic expressions. This is also the case for the position of the stagnation radius, the radius that defines the amount of matter accumulated and ejected from a cluster in the bimodal regime. Making use of these relationships and our semianalytic code (Silich et al. 2004), here we propose another interpretation of Smith's et al. (2006) observations of M82-A1, based on our bimodal solution. Our model assumes that M82-A1 is embedded in high-pressure ISM, of the thermal pressure in the core of M82 ($P/k \sim 10^7$ cm^{-3} K), which is much larger than that found in the disks of normal galaxies ($P/k \sim 10^4$ cm^{-3} K; see, e.g., Slavin & Cox 1993). Our final suggestion is that M82-A1 is a good example of a cluster evolving in the catastrophic cooling regime and that high-pressure ISM is what rapidly confines its wind, leading to its associated compact H II region.

The paper is organized as follows. In § 2 we formulate our model, and discuss the input physics and some approximations used in § 3 to develop a set of analytic equations which allow us to derive an approximate value of the heating efficiency required by the parameters of the M82-A1 cluster and its associated H II region. We confirm the analytic result by means of semianalytic calculations in § 4, where we also thoroughly discuss the structure of the outflow driven by M82-A1. In § 5 we discuss the possible impact of M82-A1, if immersed in different ISM environments. In § 6 we summarize and discuss our results.

2. M82-A1 EMBEDDED IN HIGH-PRESSURE ISM

The properties of M82-A1, in particular its mass, expected mechanical energy input rate, and the size and mass of its associated H II region, lead almost unavoidably to the conclusion that the cluster must be embedded in a high-pressure region which has managed to confine the cluster wind. This implies a rapid hydrodynamic evolution that has caused the decay of the outer shock, inhibiting the formation of an outer shell of swept-up matter and the build-up of a superbubble (as otherwise described in Weaver et al. 1977). Instead, a standing reverse shock sitting near the cluster surface decelerates and thermalizes the outflow, increasing its thermal pressure. The shocked gas then slows down while it cools and is displaced away from the cluster, as fresh wind matter enters the shock. The shocked gas thus recombines at a small distance behind the reverse shock and becomes exposed to the UV radiation from the cluster, forming a stationary H II region. Note that upon cooling, the shocked wind gas ought to undergo a rapid condensation to counterbalance the loss of temperature (from the postshock temperature to the assumed photoionization temperature $T_{H\,II} \sim 10^4$ K) and be able to keep a pressure similar to that of the surrounding ISM (P_{ISM}). In this model, the H II region associated with the central cluster results from the photoionization of three different regions. First, there is a central zone within R_{st}, where the injected matter cools in a catastrophic manner. A second photoionized zone is generated within the free wind region as this gas cools suddenly to $T_{H\,II} \sim 10^4$ K. Finally, the third zone consists of the shocked wind gas that has more recently been able to cool down from the high temperatures acquired after crossing the reverse shock. Other wind material that earlier experienced the same evolution is steadily pushed out of the standing ionized outer shell by the newly incoming material, what allows for its recombination, its further cooling by radiation, and for it to be further condensed so that its pressure remains equal to P_{ISM}.

Major restrictions on the model arise from the pressure balance between P_{ISM} and the wind ram pressure. This defines the position of the standing reverse shock, the size of the cooling distance that the shocked gas ought to travel before becoming exposed to the cluster UV radiation, which together with the available number of photons also defines the size of the outer H II region, which must agree with the observations. Here we show that to set $R_{H\,II}$ in agreement with the observations, the location of R_{sh} and the size of its cooling distance imply that M82-A1 must be experiencing a bimodal hydrodynamic solution. In the bimodal regime, strong radiative cooling largely diminishes the cluster thermal pressure within the densest central zones. This leads to the accumulation of the matter reinserted within the cooling volume, reducing the amount of mass that a cluster returns to the ISM. This also results into a slower acceleration of the matter injected into the outer segments of the cluster ($r > R_{st}$), which leads to a reduced terminal speed in the resulting wind (see Tenorio-Tagle et al. 2007; Wünsch et al. 2007). As shown below, these considerations allow us to predict which is the heating efficiency, or the fraction of the total energy input rate that is used to produce the wind of M82-A1, and which is the structure acquired by the outflow.

To derive an analytic expression for the position of the stagnation point, Wünsch et al. (2007) used the mass conservation law, together with the fact that the density at the star cluster surface scales almost linearly with that at the stagnation point. They found that for star clusters with a given radii R_{SC}, the location of the stagnation radius depends on the excess star cluster mechanical luminosity above the critical value, L_{crit}:

$$R_{st} = R_{SC}\left[1 - \left(\frac{L_{crit}}{L_{SC}}\right)^{1/2}\right]^{1/3}, \quad (1)$$

$$L_{crit} = \frac{3\pi\eta\alpha^2\mu_i^2 R_{SC} V_{A\infty}^4}{2\Lambda_{st}}\left(\frac{\eta V_{A\infty}^2}{2} - \frac{c_{st}^2}{\gamma - 1}\right), \quad (2)$$

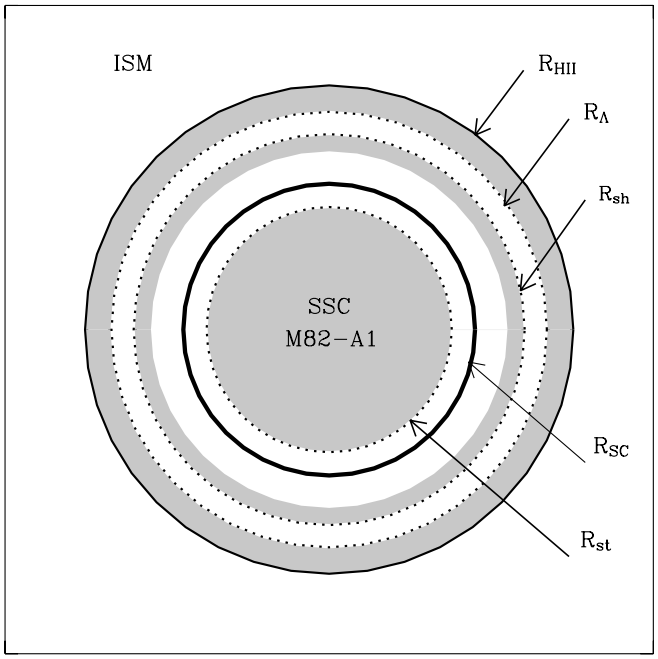

FIG. 1.—Schematic representation of the M82-A1 H II region. The ionizing cluster is contained within the radius R_{SC}. R_{st} is the stagnation radius that separates the inner cluster region, where catastrophic cooling sets in, from the outer zone ($R_{st} < r < R_{SC}$), where the thermalized ejecta remains hot and is thus able to create a stationary wind. The star cluster wind, however, cools rapidly and becomes exposed to the UV radiation from the cluster, forming a high-speed (V_∞) H II region component. Eventually this gas is stopped and reheated by the reverse shock, which sits at a fixed radius, R_{sh}, defined by the condition that the wind ram pressure equals that of the ISM. The wind processed at the reverse shock then cools down at a distance R_Λ to become once again the target of the cluster UV radiation, thus creating the outer, photoionized, thin standing shell with radius $R_{H\,II}$ (all scales are greatly distorted). The model assumes an even pressure in all regions from the ISM to the location of the reverse shock, where the wind ram pressure equals that of the ISM. Regions filled with photoionized material are shaded.

where $0 < \eta < 1$ is the heating efficiency or fraction of the deposited kinetic energy that after full thermalization is not immediately radiated away, and thus is instead evenly spread within the star cluster volume, causing the overpressure that drives the wind (Stevens & Hartwell 2003; Melioli & de Gouveia Dal Pino 2004). Here $\alpha = 0.28$ is a fiducial coefficient (see Wünsch et al. 2007), $\mu_i = 14 m_H/11$ is the mean mass per ion, $V_{A\infty} = (2 L_{SC}/\dot{M}_{SC})^{1/2}$ is the adiabatic wind terminal speed, $\dot{M}_{SC}$ is the mass deposition rate, and c_{st} and Λ_{st} are the speed of sound and the value of the cooling function at the stagnation point, respectively. Note also that the density and temperature at the stagnation radius are related by the equation (see Silich et al. 2004; Wünsch et al. 2007)

$$n_{st} = q_m^{1/2} \left[\frac{\eta V_{A\infty}^2/2 - c_{st}^2/(\gamma - 1)}{\Lambda(T_{st}, Z)} \right]^{1/2}, \quad (3)$$

where $q_m = (3\dot{M}_{SC})/(4\pi R_{SC}^3)$ is the mass deposition rate per unit volume.

Figure 1 presents a schematic representation of the model. M82-A1 is contained within the inner solid line. The dashed line inside this marks the location of the stagnation radius. Inside R_{st}, cooling dominates over the heating provided by stellar winds and supernovae. The injected matter there cools down rapidly and is unavoidably reprocessed into new generations of stars, supporting a low level of star formation as the parent cluster evolves (see Tenorio-Tagle et al. 2005).

The outer cluster zone, $R_{st} < r < R_{SC}$, is filled with hot thermalized ejecta unable to radiate away all of its thermal energy within a dynamical timescale, and thus capable of moving out of the cluster, creating a stationary wind. The amount of mass reinserted by the cluster wind is (Wünsch et al. 2007)

$$\dot{M}_{out} = \dot{M}_{SC} \left(\frac{L_{crit}}{L_{SC}} \right)^{1/2}. \quad (4)$$

Outside the cluster there is a free wind region ($R_{SC} < r < R_{sh}$) bounded by the standing reverse shock at a radius R_{sh}. The free wind is also able to cool rapidly, losing its thermal pressure while becoming an easy target of the cluster UV radiation field, and thus forming another component of the H II region associated with the cluster. At the reverse shock the ejected material, which streams with its terminal velocity V_∞, is decelerated and reheated. The matter behind R_{sh} will remain hot until it reaches the cooling radius R_Λ,

$$R_\Lambda = R_{sh} + L_\Lambda, \quad (5)$$

where the cooling length L_Λ is (Franco 1992)

$$L_\Lambda = \frac{f_\lambda V_\infty \tau_{cool}}{4} = \frac{3}{8} \frac{\mu_i}{\mu_e} \frac{k f_\lambda T_s V_\infty}{n_s \Lambda(T_s)}, \quad (6)$$

where $\mu_e = 14 m_H/23$ is the mean mass per particle in a fully ionized plasma that contains 1 helium atom per 10 atoms of hydrogen, k is the Boltzmann's constant, $T_s = 3\mu_e V_\infty^2/16k$, and $n_s = (\gamma + 1)/(\gamma - 1)\rho_w/\mu_i$ are the postshock temperature and the postshock ion density, respectively, $\Lambda(T_s)$ is the cooling function, and f_λ is a fiducial coefficient that takes into consideration the enhanced cooling promoted by the continuous growth of density in the postshock region. Good agreement between equation (6) and numerical calculations was found for $f_\lambda = 0.3$ (see below).

Outside R_Λ, the wind gas is photoionized by the UV radiation produced by the star cluster, forming a standing photoionized shell, with a pressure identical to that of the ISM.

Note that the location of the various disturbances depends only on the assumed value of P_{ISM} and on the terminal speed of the cluster wind. In this way, the density of the wind at the shock radius, ρ_w, is

$$\rho_w = P_{ram}/V_\infty^2, \quad (7)$$

where P_{ram}, the wind ram pressure, is equal to P_{ISM}. In the strongly radiative case, the terminal speed of the wind, V_∞, falls below the adiabatic value. Nevertheless, one can use the adiabatic relation between V_∞ and c_{st}, the sound speed at the stagnation point (see Cantó et al. 2000), as a good approximation that allows one to determine the radiative wind terminal speed if the sound speed at the stagnation radius is known:

$$V_\infty = \left(\frac{2 q_{eff}}{q_m} \right)^{1/2} = \left(\frac{2}{\gamma - 1} \right)^{1/2} c_{st}, \quad (8)$$

where the radiative energy losses across the cluster were assumed to be identical to those at the stagnation point. The effective energy deposition within the cluster is then

$$q_{eff} = \eta q_e - n_{st}^2 \Lambda_{st} = \frac{2}{\gamma - 1} \frac{c_{st}^2}{V_{A\infty}^2} q_e, \quad (9)$$

where q_e is the average energy deposition rate per unit volume within the cluster.

3. THE ANALYTIC MODEL

The structure of the outflow can be derived analytically from a set of equations that consider the available number of ionizing photons, the photoionization balance, the pressure confinement, and the divergence of the wind stream:

$$N^{\rm out} = f_t N^{\rm SC}, \tag{10}$$

$$R_\Lambda = R_{\rm H\,II}\left(1 - \frac{3N^{\rm out}}{4\pi\beta n_{\rm H\,II}^2 R_{\rm H\,II}^3}\right)^{1/3}, \tag{11}$$

$$\rho_w(R_{\rm sh})V_\infty^2 = P_{\rm ISM}, \tag{12}$$

$$\rho_w(R_{\rm sh}) = \frac{\dot{M}_{\rm out}}{4\pi R_{\rm sh}^2 V_\infty}, \tag{13}$$

where $\beta = 2.59\times10^{-13}$ cm^{-3} s^{-1} is the recombination coefficient to all but the ground level, $N^{\rm SC}$ is the total number of UV photons produced by the cluster, and $N^{\rm out}$ is the total number of photons escaping the cluster and the free wind region, and thus available to impact on the shocked wind gas once this has cooled by radiation and has acquired a density $n_{\rm H\,II}$ through condensation. The stagnation radius, $R_{\rm st}$, and the amount of matter that a cluster returns to the ISM, $\dot{M}_{\rm out}$, are defined by equations (1), (2), and (4). The term f_t is the fraction of the star cluster ionizing radiation that reaches the cool shocked gas behind the standing reverse shock. Combining equations (11) and (5), one can derive the expression for the reverse shock radius, $R_{\rm sh}$:

$$R_{\rm sh} = R_{\rm H\,II}\left(1 - \frac{3N^{\rm out}}{4\pi\beta n_{\rm H\,II}^2 R_{\rm H\,II}^3}\right)^{1/3} - \frac{3}{8}\frac{\mu_i}{\mu_e}\frac{kf_\lambda T_s V_\infty}{n_s\Lambda(T_s)}. \tag{14}$$

On the other hand, the position of the reverse shock is defined by the equations of mass conservation (eq. [13]) and pressure balance (eq. [12]), and by the amount of mass that the cluster returns to the ISM (eq. [4]):

$$R_{\rm sh} = \left(\frac{\dot{M}_{\rm out}V_\infty}{4\pi P_{\rm ISM}}\right)^{1/2} = \frac{(4L_{\rm crit}L_{\rm SC}V_\infty^2)^{1/4}}{(4\pi P_{\rm ISM}V_{A\infty}^2)^{1/2}}, \tag{15}$$

where V_∞ and $V_{A\infty}$ are the radiative and adiabatic wind terminal speeds, respectively (see Wünsch et al. 2007).

Substituting equation (15) into equation (14), we obtain a nonlinear algebraic equation that defines the heating efficiency, η, required to match the observed parameters of the H II region ($R_{\rm H\,II}$, $N^{\rm obs}$) associated with M82-A1, if one accounts for the star cluster parameters ($R_{\rm SC}$, $L_{\rm SC}$) and the inferred pressure of the ISM,

$$1 - \frac{(4\pi P_{\rm ISM}V_{A\infty}^2 R_{\rm H\,II}^2)^{1/2}}{(4L_{\rm crit}L_{\rm SC}V_\infty^2)^{1/4}} \times\left[\left(1 - \frac{3f_t N^{\rm SC}}{4\pi\beta n_{\rm H\,II}^2 R_{\rm H\,II}^3}\right)^{1/3} - \frac{9}{512}\frac{f_\lambda\mu_i^2 V_\infty^5}{P_{\rm ISM}R_{\rm H\,II}\Lambda(T_s)}\right] = 0. \tag{16}$$

If the adiabatic wind terminal speed, $V_{A\infty}$, is known, the only free parameter in equation (16) is $0 < f_t < 1$, the fraction of UV photons able to reach the outer H II region. One can then solve equation (16) by iterations for a given value of f_t.

The solution of equation (16) shows that the heating efficiency required in order to fit the observed structure of the M82-A1 H II region is small, $\eta \approx 4.65\%$, and does not depend significantly on the adopted value of f_t. Figure 2 displays the structure of the outflow produced by M82-A1, as well as the dimensions of its associated outer H II region, calculated under the assumption that $V_{A\infty} = 1000$ km s^{-1}. The low value of the heating efficiency results in a large stagnation radius ($R_{\rm st} \approx 2.94$ pc; lower solid line in Fig. 2), which implies that a large fraction of the matter supplied by stellar winds and supernovae will remain bound to the cluster, and thus only the small amount deposited between $R_{\rm st}$ and $R_{\rm SC}$ will form the cluster wind, while expanding at approximately 200 km s^{-1}. The outflow is strongly decelerated and reheated at the reverse shock (4.24 pc $\leq R_{\rm sh} \leq$ 4.35 pc; second solid line from the bottom in Fig. 2), and then cools down rapidly to form an outer shell of photoionized matter, depleting the photons that escape the cluster ($N^{\rm out}$). Note that the thickness of this outer shell is very small, and becomes even smaller as one assumes a smaller number of photons escaping the SSC and the cluster wind.

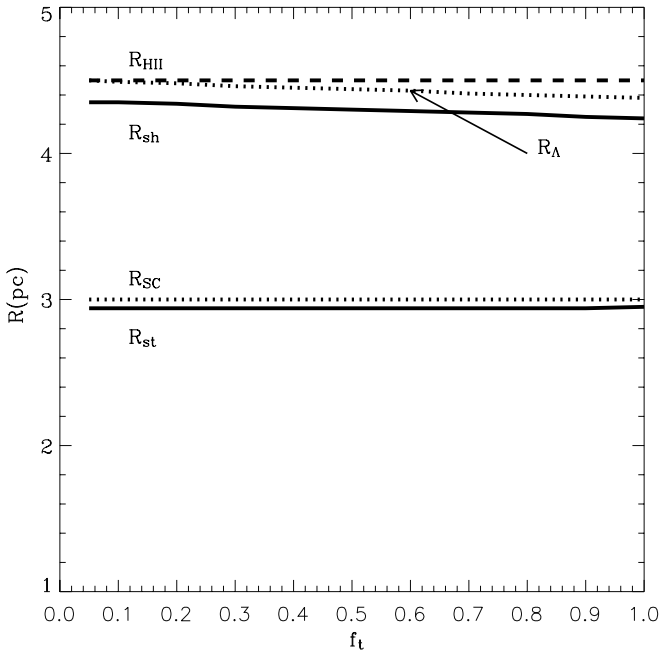

FIG. 2.—Analytic model of M82-A1 and its associated H II region. The various lines mark the locations of different hydrodynamical disturbances as a function of f_t. From bottom to top these represent the location of the stagnation radius ($R_{\rm st}$), the cluster radius ($R_{\rm SC}$), the reverse shock location ($R_{\rm sh}$), the cooling radius (R_Λ), and the outer radius of the standing H II region ($R_{\rm H\,II}$).

4. THE SEMIANALYTIC MODEL

To corroborate our results, here we use our semianalytic code (see Silich et al. 2004), which accurately calculates the divergent spherically symmetric outflow beyond $R_{\rm st}$, accounting for strong radiative cooling.

We use first the trial heating efficiency η to calculate the position of the stagnation point, as suggested in Tenorio-Tagle et al. (2007), and then integrate the equations of mass, momentum, and energy conservation outward, knowing that at some distance from the cluster the standing reverse shock sets in. We stop the integration at the reverse shock, and use then the Rankine-Hugoniot conditions to calculate the thermal pressure and the velocity of the plasma behind the shock front:

$$P_2 = P_w\left[\frac{2\gamma M_1^2 - (\gamma-1)}{\gamma+1}\right], \tag{17}$$

$$u_2 = u_w\left(\frac{\gamma-1}{\gamma+1} + \frac{2}{\gamma+1}\frac{1}{M_1^2}\right), \tag{18}$$

where P_w, u_w and P_2, u_2 are the thermal pressure and the velocity of the outflow ahead of and behind the reverse shock, respectively, $M_1 = u_w/c_w$ is the Mach number ahead of the shock front, and $\gamma = 5/3$ is the ratio of specific heats. P_2 and u_2, together with the mass conservation law, $\dot{M}_{\rm out} = 4\pi\rho_w u_w R_{\rm sh}^2$, define the initial conditions behind the reverse shock for the set of main equations outside of the cluster (see Silich et al. 2004):

$$\frac{du_w}{dr} = \frac{1}{\rho_w}\frac{(\gamma-1)rQ + 2\gamma u_w P_w}{r(u_w^2 - c_s^2)}, \quad (19)$$

$$\frac{dP_w}{dr} = -\frac{\dot{M}_{\rm out}}{4\pi r^2}\frac{du_w}{dr}, \quad (20)$$

$$\rho_w = \frac{\dot{M}_{\rm out}}{4\pi u_w r^2}. \quad (21)$$

The run of the hydrodynamical variables in the outer part of the flow was obtained by integrating equations (19)–(21) from the reverse shock radius outwards.

The thermal pressure, P_w, and the wind expansion velocity, u_w, ahead of the shock front depend on the star cluster parameters and on the radius of the reverse shock, $R_{\rm sh}$. Therefore, the set of initial conditions (17)–(18) contains two model parameters: the value of the heating efficiency, η, and the position of the reverse shock, $R_{\rm sh}$. We iterate η and $R_{\rm sh}$ until the conditions

$$R_\Lambda = R_{\rm H\,II}\left(1 - \frac{3N^{\rm out}}{4\pi\beta n_{\rm H\,II}^2 R_{\rm H\,II}^3}\right)^{1/3}, \quad (22)$$

$$P_{\rm H\,II} = P_{\rm ISM}, \quad (23)$$

are fulfilled. Here $R_{\rm H\,II} = 4.5$ pc is the observed radius of the M82-A1 H II region, and $P_{\rm H\,II} = k\,n_{\rm H\,II}T_{\rm H\,II}$ and $T_{\rm H\,II} = 10^4$ K are the thermal pressure and the temperature of the ionized gas in the standing outer shell, respectively.

Figure 3 presents the results of the calculation assuming $f_t = 0.5$, e.g., when only half of the ionizing photons reach the outer standing shell. The expansion velocity of the outflow grows from zero at the stagnation radius to rapidly reach its terminal value, $V_\infty \approx 180$ km s^{-1}, and then drops when the free wind reaches the reverse shock at $r \approx 4.4$ pc (Fig. 3*a*). The gas decelerates rapidly at the reverse shock, and as it cools down it is further condensed. Thus, in the case of the pressure-confined wind, the reverse shock separates gas that flows supersonically in the free wind region from gas moving away with a subsonic velocity. The thermal pressure (see Fig. 3*b*) drops initially when the gas is accelerated to reach its terminal speed, and remains at its lowest value as a consequence of radiative cooling. The $P_{\rm th}$ is restored after crossing the reverse shock, where the ram pressure in the free wind reaches a balance with the thermal pressure in the surrounding interstellar medium, and after photoionization of the dense outer layer. The density decreases as r^{-2} in the free wind region. It is then compressed at the shock, and reaches the H II region value upon condensation induced by radiative cooling, and finally the maximum value in the neutral layer outside of the outer photoionized shell (Fig. 3*c*). Figure 3 also shows that in the bimodal regime the temperature of the outflowing matter drops rapidly outside of the cluster. The free wind is then reheated at the reverse shock and cools down again to form the outer shell whose inner skin is photoionized by the Lyman continuum escaping from the M82-A1 cluster. Note that in our calculations the temperature of the free wind (between the star cluster surface and the reverse shock) drops to 10^4 K, and thus a broad ($u_w \approx 180$ km s^{-1}), low-intensity emission-line component is expected from this region.

Certainly, the analytic model is unable to show any detailed structure of the outflow. Nevertheless, the analytic heating efficiency, stagnation radius, reverse shock, and cooling radii are in reasonable agreement with the results obtained from the semianalytic model: $\eta = 6.8\%$, $R_{\rm st} = 2.86$ pc, $R_{\rm sh} = 4.41$ pc, and $R_\Lambda = 4.45$ pc, if the fraction of ionizing photons reaching the outer H II region is $f_t = 0.5$.

5. M82-A1 IN DIFFERENT ENVIRONMENTS

The theory developed in the previous sections is based on the assumption that the H II region detected around the M82-A1 is a standing, photoionized shell of shocked wind matter, confined by the high pressure of the ISM. One major implication of the results above is that clusters with properties (size, mass, and age) similar to those of M82-A1 would have a low heating efficiency. Here we assume such a cluster to be embedded in different ISM environments and work out the properties of the resulting pressure-confined remnant.

The different pressure in the ambient ISM does not affect the distribution of matter within the cluster. It would not affect the position of the stagnation radius, nor the density, temperature, or velocity of the ejected plasma. A different ISM pressure would modify only the outer structure of the outflow, shifting the position of the reverse shock. This is because of the pressure equilibrium condition, $P_{\rm ram} = \rho_w(R_{\rm sh})V_\infty^2 = P_{\rm H\,II} = P_{\rm ISM}$. Using equations (4) and (13), one can obtain the position of the reverse shock for M82-A1 sitting in different interstellar environments:

$$R_{\rm sh} = \left(\frac{\dot{M}_{\rm out}V_\infty}{4\pi P_{\rm ISM}}\right)^{1/2} = \left(\frac{\dot{M}_{\rm SC}V_\infty}{4\pi P_{\rm ISM}}\right)^{1/2}\left(\frac{L_{\rm crit}}{L_{\rm SC}}\right)^{1/4}. \quad (24)$$

One can then find the outer radius of the H II region from equations (5), (6), and (11), knowing that the density in the ionized outer shell is a linear function of the pressure in the ambient interstellar medium,

$$n_{\rm H\,II} = P_{\rm ISM}/kT_{\rm H\,II}, \quad (25)$$

where the temperature of the photoionized shell, $T_{\rm H\,II}$, is set through photoionization and therefore does not depend on $P_{\rm ISM}$. Equation (24) also indicates that there exists a critical interstellar pressure, $P_{\rm crit}$,

$$P_{\rm crit} = \frac{\dot{M}_{\rm SC}V_\infty}{4\pi R_{\rm SC}^2}\left(\frac{L_{\rm crit}}{L_{\rm SC}}\right)^{1/2}. \quad (26)$$

If the pressure in the ambient ISM exceeds this critical value, $P_{\rm ISM} > P_{\rm crit}$, the cluster will not have sufficient power to drive a cluster wind. In this case, all matter deposited by stellar winds and SNe would remain buried within the cluster.

Figure 4 shows the structure of the pressure-confined remnants that M82-A1 would produce in different interstellar environments. Our results show that the outer ionized shell is very thin, and that the radius of the ionized shell shrinks toward the star cluster if one considers a pressure in the interstellar medium that approaches the critical value (eq. [26]), and grows as the pressure in the interstellar medium drops. The analytic results (Fig. 4, *dashed and dotted lines*) show reasonable agreement with those obtained by semianalytic calculations (Fig. 4, *crosses*).

6. RESULTS AND DISCUSSION

The results from our analytic formulation of a pressure-confined wind, in agreement with those obtained with our semianalytical

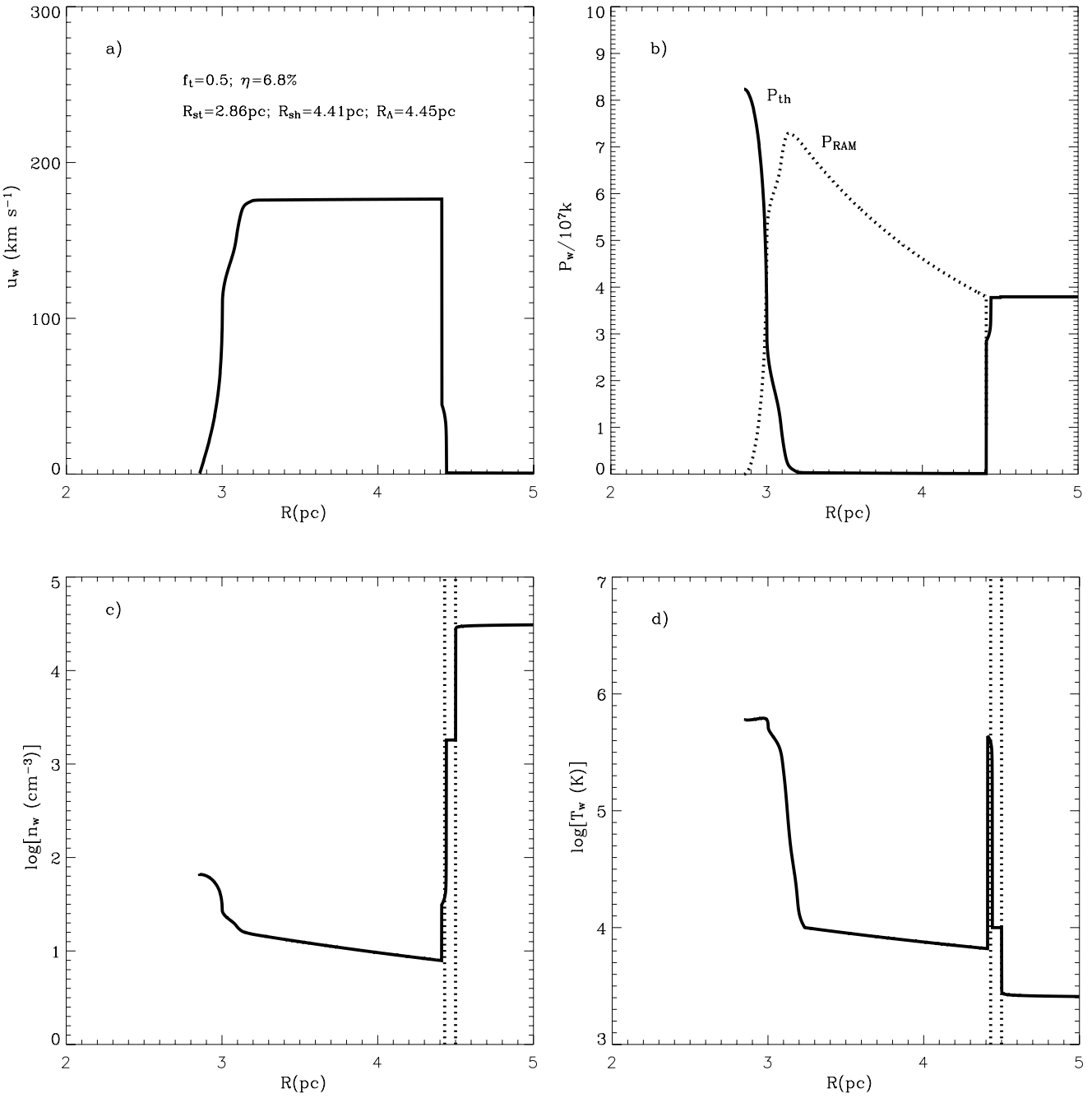

FIG. 3.— Semianalytic model of M82-A1 and its associated H II region. Panels *a*–*d* present the distributions of the velocity, thermal (*solid line*) and ram (*dotted line*) pressures, density, and temperature, respectively. The size of the standing outer H II region is indicated in panels *c* and *d* by the two vertical dotted lines. The calculations assumed $f_i = 0.5$, $Z = Z_\odot$, and an adiabatic wind terminal speed, $V_{A\infty} = 1000$ km s^{-1}.

code, imply that M82-A1 is a massive and compact cluster with a low heating efficiency. This implies a completely different result from what one would expect from an adiabatic model, as a low heating efficiency leads to a bimodal hydrodynamic solution, and with it a low mass deposition rate into the ISM, with a much reduced outflow velocity.

Furthermore, to match the observed parameters of M82-A1 and its associated H II region, our results also suggest a high-pressure environment able to confine the cluster wind by setting a reverse shock close to the star cluster surface. In this way the outflow is thermalized, which leads to temperatures near the top of the interstellar cooling curve, and thus to a rapid cooling of the strongly decelerated outflow. The wind then becomes a target for the cluster UV radiation, forming a narrow standing outer shell of photoionized gas with the shocked wind matter that continuously traverses the reverse shock.

Our calculations lead to three H II region components associated with M82-A1: (1) a central component where the deposited matter cools catastrophically and does not participate in the wind, (2) a section of the free wind region which, on expansion, is also able to cool rapidly, and (3) the outer stationary shell of shocked wind matter, which defines the observed size of the associated H II region. Note that, given the densities in the latter component, it ought to produce the most intense emission lines, while the second component should produce a broad ($2V_\infty$) low-intensity emission-line component, similar to that detected in NGC 4214-1

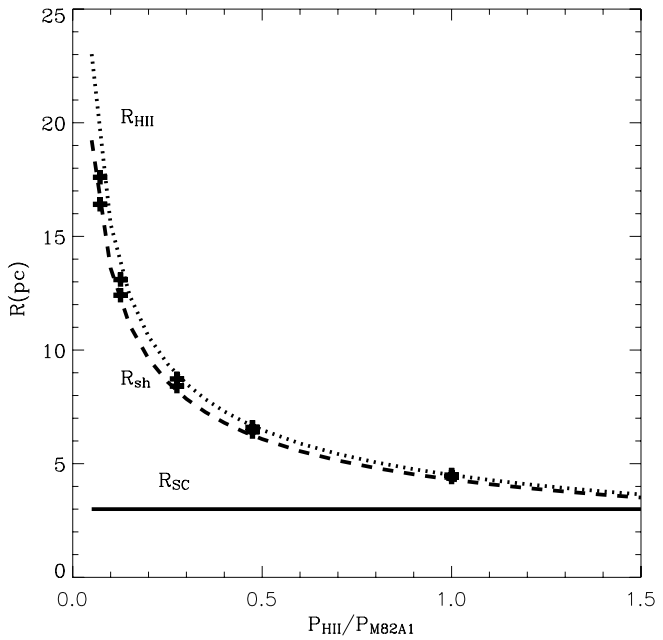

FIG. 4.— Structure of pressure-confined winds in different ISM environments. We have assumed the star cluster parameters derived by Smith et al. (2006) for M82-A1 and a heating efficiency $\eta = 4.6\%$, as derived in § 3. The solid line marks the star cluster radius that is equal to the half-light radius of M82-A1. The dashed and dotted lines mark the position of the reverse shock, $R_{\rm sh}$, and of the outer H II region, $R_{\rm H\,II}$, respectively, as a function of $P_{\rm ISM}$ normalized to that found by Smith et al. (2006) in the M82-A1 H II region. The crosses show the results of the semianalytic calculations and also mark the positions of the shock front and the outer edge of the H II region (*lower and upper symbols, respectively*). The fraction of the star cluster ionizing radiation able to photoionize the outer shell is $f_i = 0.5$ in both the analytic and semianalytic calculations.

(see Ho & Filippenko 1996), which would be able to enhance the width of the observed lines, as in the case of M82-A1. Our two methods have also shown good agreement when considering the wind of M82-A1 as pressure confined by ISM with different pressures.

Note that in the case of very young SSCs (a few Myr old), their mass is usually derived from the intensity of their optical emission lines, which emanate from their associated compact H II regions, and thus is arrived at through a measurement of the available UV photon flux, via an assumed IMF and stellar synthesis models (Melo et al. 2005; Smith et al. 2006). In the light of the models presented here, this implies that young SSCs are embedded in a high-pressure ISM, and also that their heating efficiency ought to be rather small, in order for their winds to be pressure confined in the immediate neighborhood of the clusters, and thus to present an associated low-mass, compact H II region.

Note also that the two different populations of massive and compact clusters (Gyr old and very young clusters) present a similar range of masses as well as a similar size distribution. This can be explained if most of the mass reinserted by stellar winds and supernova explosions during the early evolutionary stages (which may amount to 30% of the $M_{\rm SC}$ released during the first 50 Myr of evolution) is not returned to the ISM but rather reprocessed in situ into further stellar generations. This would allow SSCs to keep most of their mass (and size) as they age. This also implies that a large fraction of the low-mass stars currently observed in old compact and massive stellar clusters might have formed from matter injected by massive stars. In this respect, our bimodal model provides the hydrodynamical grounds for self-enrichment scenarios. In these, for example, the abundance anomalies observed in globular clusters may result from the enrichment of the protostellar gas during the earlier stages of their evolution (see, e.g., Prantzos & Charbonnel 2006; Decressin et al. 2007 for a comprehensive discussion of different aspects of this problem). Our solution also suggests that the metallicity of the compact H II regions associated with intermediate-age (5–10 Myr) massive clusters should be supersolar and variable with time.

We thank our anonymous referee for valuable comments and suggestions. This study has been supported by CONACYT-México, research grant 47534-F and AYA2004-08260-CO3-O1 from the Spanish Consejo Superior de Investigaciones Científicas.

REFERENCES

Bisnovatyi-Kogan, G. S., & Silich, S. A. 1995, Rev. Mod. Phys., 67, 661
Cantó, J., Raga, A. C., & Rodriguez, L. F. 2000, ApJ, 536, 896
Chevalier, R. A., & Clegg, A. W. 1985, Nature, 317, 44
Decressin, T., Meynet, G., Charbonnel, C., Prantzos, N., & Ekström, S. 2007, A&A, 464, 1029
de Grijs, R., O'Connell, R. W., & Gallagher, J. S. 2001, AJ, 121, 768
Dopita, M. A., Groves, B. A., Fischera, J., et al. 2005, ApJ, 619, 755
Franco, J. 1992, in Star Formation in Stellar Systems III, ed. G. Tenorio-Tagle, M. Prieto, & F. Sánches (Cambridge: Cambridge Univ. Press), 515
Ho, L. C. 1997, Rev. Mex. AA Ser. Conf., 6, 5
Ho, L. C., & Filippenko, A. V. 1996, ApJ, 472, 600
Kewley, L. J., & Dopita, M. A. 2002, ApJS, 142, 35
Larsen, S. S. 2006, in Planets to Cosmology, ed. M. Livio (Cambridge: Cambridge Univ. Press), 35
Leitherer, C., Schaerer, D., Goldader, J. D., et al. 1999, ApJS, 123, 3
Martín-Hernández, N. L., Schaerer, D., & Sauvage, M. 2005, A&A, 429, 449
McCrady, N., Gilbert, A. M., & Graham, J. R. 2003, ApJ, 596, 240
Melioli, C., & de Gouveia Del Pino, E. M. 2004, A&A, 424, 817
Melo, V. P., Muñoz-Tuñón, C., Maíz-Apellániz, J., & Tenorio-Tagle, G. 2005, ApJ, 619, 270
Muñoz-Tuñón, C., Tenorio-Tagle, G., Melo, V., Silich, S., & Maiz-Apellániz, J. 2004, in ASP Conf. Ser. 322, The Formation and Evolution of Massive Young Clusters (San Francisco: ASP), 191
Pasquali, A., Gallagher, J. S., & de Grijs, R. 2004, A&A, 415, 103
Prantzos, N., & Charbonnel, C. 2006, A&A, 458, 135
Silich, S., Tenorio-Tagle, G., & Rodríguez González, A. 2004, ApJ, 610, 226 (Paper I)
Slavin,, J. D., & Cox, D. P. 1993, ApJ, 417, 187
Smith, L. J., Westmoquette, M. S., Gallagher, J. S. III, O'Connell, R. W., Rosario, D. J., & de Grijs, R. 2006, MNRAS, 370, 513
Stevens, I. R., & Hartwell, J. M. 2003, MNRAS, 339, 280
Tenorio-Tagle, G., Silich, S., Rodríguez-González, A., & Muñoz-Tuñon, C. 2005, ApJ, 628, L13 (Paper II)
Tenorio-Tagle, G., Wünsch, R., Silich, S., & Palouš, J. 2007, ApJ, 658, 1196 (Paper III)
Thompson, R. I., Sauvage, M., Kennicutt, R. C., & Engelbracht, C. W. 2006, ApJ, 638, 176
Turner, J. L., & Beck, S. C. 2004, ApJ, 602, L85
Turner, J. L., Beck, S. C., Crosthwaite, L. P., et al. 2003, Nature, 423, 621
Walcher, C. J., van der Marel, R. P., McLaughlin, D., Rix, H.-W., Böker, T., Häring, N., Ho, L. C., Sarzi, M., & Shields, J. C. 2005, ApJ, 618, 237
Weaver, R., McCray, R., Castor, J., Shapiro, P., & Moore, R. 1977, ApJ, 218, 377
Whitmore, B. C. 2003, in A Decade of HST Science, ed. M. Livio, K. Noll & M. Stiavelli (Cambridge: Cambridge Univ. Press), 153
Wünsch, R., Silich, S. Palouš, J., & Tenorio-Tagle, G. 2007, A&A, 471, 579